Inorganic Chemistry

Article

pubs.acs.org/IC

# Step-by-Step Introduction of Silazane Moieties at Ruthenium: Different Extents of Ru−H−Si Bond Activation

Katharine A. Smart,[†,‡] Mary Grellier,*[,†,‡] Laure Vendier,[†,‡] Sax A. Mason,[§] Silvia C. Capelli,[§] Alberto Albinati,[∥] and Sylviane Sabo-Etienne*[,†,‡]

[†]LCC (Laboratoire de Chimie de Coordination), CNRS, 205 Route de Narbonne, F-31077 Toulouse, France

[‡]Université de Toulouse, UPS, INPT, F-31077 Toulouse, France

[§]Institut Laue-Langevin, 6 rue Jules Horowitz, BP 156, 38042 Grenoble Cedex 9, France

[∥]Dipartimento di Chimica, Università di Milano, Via C. Golgi, 19, 20133 Milan, Italy

Supporting Information

**ABSTRACT:** The coordination of pyridine-2-amino(methyl)-dimethylsilane ligands to ruthenium has afforded access to a family of novel complexes that display multicenter Ru−H−Si interactions according to the number of incorporated ligands. The new complexes Ru[κ-Si,N-(SiMe$_2$)N(Me)(C$_5$H$_4$N)]($\eta^4$-C$_8$H$_{12}$)($\eta^3$-C$_8$H$_{11}$) (**1**), Ru$_2$($\mu$-H)$_2$(H)$_2$[κ-Si,N-(SiMe$_2$)N-(Me)(C$_5$H$_4$N)]$_4$ (**2**), and Ru(H)[κ-Si,N-(SiMe$_2$)N(Me)-(C$_5$H$_4$N)]$_3$ (**3**) were isolated and fully characterized. The complexes exhibit different degrees of Si−H activation: complete Si−H cleavage, secondary interactions between the atoms (SISHA), and $\eta^2$-Si−H coordination. Reversible protonation of **3** leading to the cationic complex [RuH{($\eta^2$-H-SiMe$_2$)N(Me)κ-N-(C$_5$H$_4$N)}{κ-Si,N-(SiMe$_2$)N(Me)(C$_5$H$_4$N)}$_2$]$^+$[BAr$^F_4$]$^-$ (**5**) was also demonstrated. The coordination modes in these systems were carefully studied with a combination of X-ray and neutron diffraction analysis, DFT geometry optimization, and multinuclear NMR spectroscopy.

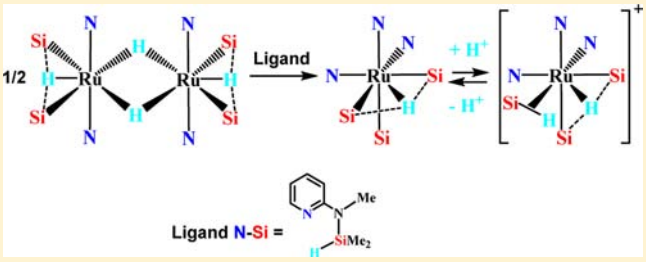


## INTRODUCTION

Silazane (R$_3$Si)$_n$N(R′)$_{3-n}$ compounds are implicated in many domains, from organic chemistry to materials science.[1] Silazane derivatives bearing a Si−H function can offer additional multicenter properties, but except for the area of ceramics where they serve as precursors for the preparation of polymer-derived ceramics, their chemistry remains relatively unexplored.[2] Recently, Sadow and co-workers reported the magnesium-catalyzed formation of Si−N bonds, promoting the method as an alternative to the substitution reaction of chlorosilanes with amines that is often employed in the synthesis of silazanes.[2a] Silazanes employed as ligands have been shown by Nolan, Thomas, and co-workers to increase the activity of gold catalysts in the polymerization of *rac*-β-butyrolactone.[2e] In the field of materials, the spectroscopic properties of the Si−H bonds of silazanes were for example exploited by Anwander and co-workers in the characterization of iron silylamide-grafted periodic mesoporous silica.[1c]

We entered this field with the commercial disilazane compound, (Me$_2$HSi)$_2$NH, and achieved catalytic, selective deuteration to give (Me$_2$DSi)$_2$NH. Moreover, we showed that (Me$_2$HSi)$_2$NH could substitute the two labile dihydrogen ligands in RuH$_2$(H$_2$)$_2$(PCy$_3$)$_2$ to form the corresponding disilazane complex RuH$_2${($\eta^2$-HSiMe$_2$)$_2$NH}(PCy$_3$)$_2$ stabilized by secondary interactions between the hydrides and the silicon atoms (SISHA).[3] In contrast, the coordination of the pyridine-substituted compound, 2-pyridinetetramethyldisilazane, to the two ruthenium complexes RuH$_2$(H$_2$)$_2$(PCy$_3$)$_2$ and its precursor Ru($\eta^4$-C$_8$H$_{12}$)($\eta^6$-C$_8$H$_{10}$) gave rise to the formation of mononuclear complexes with dangling Si−H bonds and pyridine coordination to the ruthenium.[4] Clearly modification of the N-substituent of silazanes is a means of achieving novel complexes displaying a large variety of coordination modes where it is possible to modulate Si−H bond activation. Comprehensive understanding of Si−H activation by metal centers is indeed crucial for the tuning of catalytic processes such as hydrosilylation.[5] In the present work we focus on the use of pyridine-2-amino(methyl)dimethylsilane to prepare mononuclear and dinuclear ruthenium compounds incorporating one, two, or three silazane ligands in a stepwise manner. The compounds exhibit a range of multicenter Ru−H−Si bonding, from Si−H cleavage to Si$_2$−H, Si$_3$−H, and [Si$_3$−H$_2$]$^+$ interactions, and we show that reversible protonation can be achieved. The nature of the bonding in these dynamic systems has been delineated with a combination of multinuclear NMR spectroscopy, DFT, X-ray, and neutron structural determinations.

**Received:** December 6, 2012
**Published:** February 19, 2013

   dx.doi.org/10.1021/ic302682f | Inorg. Chem. 2013, 52, 2654−2661

**Scheme 1. Step by Step Synthesis of Complexes 1−3**

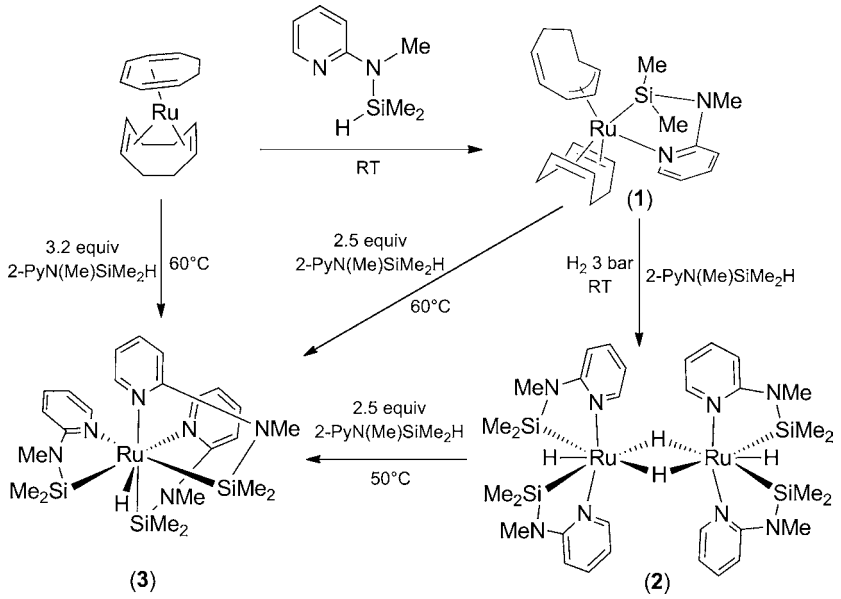


## RESULTS AND DISCUSSION

**Synthesis of Complexes 1−3.** Addition of pyridine-2-amino(methyl)dimethylsilane to a solution of Ru($\eta^4$-$C_8H_{12}$)-($\eta^6$-$C_8H_{10}$) led to the formation of Ru[$\kappa$-Si,N-(SiMe$_2$)N(Me)-($C_5H_4N$)]($\eta^4$-$C_8H_{12}$)($\eta^3$-$C_8H_{11}$) (**1**) (Scheme 1), which was isolated as a pale yellow powder in 81% yield and characterized by NMR spectroscopy and X-ray diffraction. Compound **1** results from the coordination of the silazane, through Si−H bond cleavage inducing the reduction of cyclooctatriene to form an $\eta^3$-allyl system. Heteronuclear (H,C)-single quantum coherence (HSQC) NMR spectroscopy enabled assignment of the ligands around the metal center. The $^1$H NMR spectrum of **1** has a relatively high field signal at $\delta$ = −0.02 ppm for one of the protons in the $\eta^3$-$C_8H_{11}$ ring. A $^{29}$Si singlet at $\delta$ = 81.0 ppm is observed in the gradient-pulsed heteronuclear (H,Si)-multiple quantum coherence (HMQC) NMR spectrum of **1**, which can be compared to $\delta$ = −4.14 for the free ligand. The three carbon atoms of the allyl system resonate at $\delta$ 58.55, $\delta$ 106.85, and $\delta$ 70.03. As expected, the central allyl carbon is the most deshielded.[6] The adjacent unsaturated carbons, which do not have a bonding interaction with the ruthenium atom, are found at $\delta$ 137.07 and $\delta$ 123.89. The two nitrogen environments are distinguished by (H,N)-HMQC NMR spectroscopy with $\delta$ = −168.7 ppm for the coordinating pyridinic nitrogen and $\delta$ = −282.9 ppm for the amino nitrogen, comparable with −104.4 ppm and −312.2 ppm for the corresponding nitrogen atoms in the free ligand. The X-ray structure of **1** is depicted in Figure 1, and geometrical parameters are listed in Table 1. The carbon−carbon bond lengths of the $C_8H_{11}$ ligand are indicative of five adjacent unsaturated carbon atoms (C17−21), with three of these carbon atoms (C17−19) providing an $\eta^3$-bonding interaction with ruthenium. The Ru−C allylic (C17−19) distances of **1** are 2.282(2), 2.227(2), and 2.442(2) Å. The presence of a C=C bond adjacent to the coordinated allyl moiety might be responsible for the lengthening of the Ru−C19 distance. For comparison, in [$\kappa^2$P,P′-{($\eta^3$-$C_6H_8$)CyP($CH_2$)$_3$PCy$_2$}Ru($\eta^3$-$C_8H_{13}$)] the corresponding Ru−C allylic distances are 2.270(4), 2.151(3), and 2.311(4).[6a] This instance in **1** of $\eta^3$-coordination of five adjacent unsaturated carbon atoms to a metal center is, to the best of our knowledge, unique.

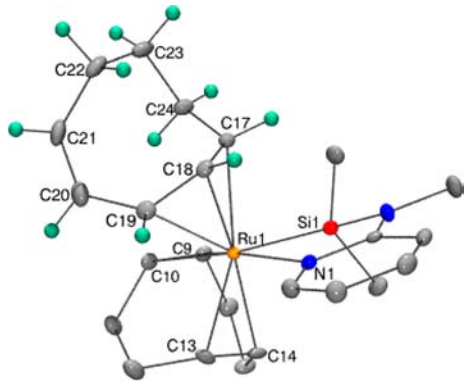


**Figure 1.** X-ray molecular structure of **1** (50% probability ellipsoids with hydrogen atoms represented by green spheres or excluded for clarity).

**Table 1. Selected Bond Distances (Å) and Angles (deg) for 1**

| | | | |
|---|---|---|---|
| C9−C10 | 1.410(3) | Ru−C9 | 2.227(2) |
| C13−C14 | 1.415(3) | Ru−C10 | 2.207(2) |
| C17−C18 | 1.426(3) | Ru−C13 | 2.189(2) |
| C18−C19 | 1.414(3) | Ru−C14 | 2.195(2) |
| C19−C20 | 1.479(3) | Ru−C17 | 2.282(2) |
| C20−C21 | 1.325(4) | Ru−C18 | 2.227(2) |
| C21−C22 | 1.522(4) | Ru−C19 | 2.442(2) |
| C22−C23 | 1.542(4) | Ru−Si | 2.3809(7) |
| C23−C24 | 1.543(3) | Ru−N1 | 2.188(2) |
| Si−Ru−N1 | 78.76(5) | | |

The reaction of **1** with an equivalent of pyridine-2-amino(methyl)dimethylsilane under a pressure of 3 bar of $H_2$ yielded the dinuclear complex Ru$_2$($\mu$-H)$_2$(H)$_2$[$\kappa$-Si,N-(SiMe$_2$)-N(Me)($C_5H_4N$)]$_4$ (**2**) (Scheme 1), which was isolated as a red powder in 22% yield and characterized by NMR and infrared spectroscopy, and X-ray diffraction. The $^1$H NMR integration ratios are consistent with the presence of two bridging and two terminal hydrides in comparison to four silazane ligands. The


dx.doi.org/10.1021/ic302682f | Inorg. Chem. 2013, 52, 2654−2661

two high field triplet signals, at $\delta = -1.32$ ppm ($^2J_{HH} = 7.1$ Hz) and $\delta = -9.66$ ppm with $^{29}$Si satellites ($^2J_{HH} = 7.2$ Hz, $J_{HSiapp} = 28.0$ Hz), are attributed to the bridging and terminal hydrides, respectively. A single singlet at $\delta = 51.5$ ppm observed in the (H,Si)-HMQC NMR spectra of **2** at room temperature and at 193 K indicates that the four silicon atoms are equivalent in solution. The (H,N)-HMQC NMR spectrum distinguishes the two nitrogen environments: $\delta = -171.9$ ppm for the coordinating pyridinic nitrogen and $\delta = -287.1$ ppm for the amino nitrogen. The X-ray structure of **2** is depicted in Figure 2, and the geometrical parameters are given in Table 2.

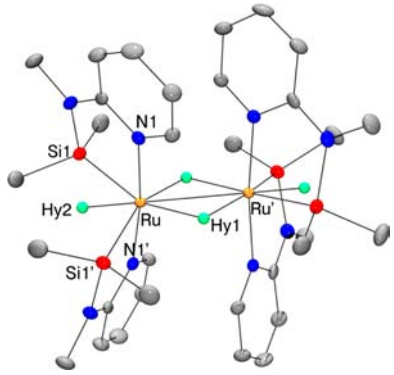


**Figure 2.** X-ray molecular structure of **2** (ellipsoids are shown at 50% probability with hydrogen atoms represented by green spheres or excluded for clarity.).

**Table 2. Selected Bond Distances (Å) and Angles (deg) for 2**

| | | | |
|---|---|---|---|
| N1−Ru | 2.112(1) | Si−Hy2 | 1.96(2) |
| Si−Ru | 2.3283(5) | N1−Ru−N1′ | 173.14(7) |
| Ru−Ru′ | 2.8850(3) | N1−Ru−Si | 81.93(4) |
| Ru−Hy1 | 1.80(2) | Si−Ru−Si′ | 113.01(3) |
| Ru−Hy2 | 1.51(3) | | |

Complex **2** possesses a motif unusual in ruthenium chemistry, namely two bridging hydrides together with two terminal hydrides positioned between two silyl groups. The only other ruthenium complex with two bridging and two terminal hydrides to be found on searching the Cambridge Structural Database is $Ru_2H_4(PMe_3)_6$, although here not all of the hydrides were located.[7] The asymmetric unit of **2** contains a single Ru−Si−$(H)_2$ moiety, and the dimeric bridged structure is generated from the symmetry elements of the $P4_22_12$ space group. The terminal hydrides of **2** are located in the same plane as Ru($\mu$-H)$_2$Ru as confirmed by DFT optimization. The terminal hydrides are equidistant between the silicon atoms with a relatively short silicon−hydride distance of 1.96(2) Å (1.996 Å by DFT), which implies the presence of "strong" secondary interactions (SISHA).[8] The expected range for SISHA is 1.9−2.4 Å. Further evidence for a rather strong Si−H interaction is provided by the relatively large coupling constant $J_{HSiapp} = 28.0$ Hz.[9] $\eta^2$-Si−H coordination to a metal center results in reduced $J_{SiH}$ values relative to an unbound silane (ca. 200 Hz), and it is generally considered that values lower than 20 Hz are characteristic of very weak interactions. For small values (a few Hz) oxidative addition can be inferred.[5a,9,10]

Reaction of **1** with 2.5 equiv of pyridine-2-amino(methyl)-dimethylsilane at 60 °C leads to Ru(H)[$\kappa$-Si,N-(SiMe$_2$)N-(Me)(C$_5$H$_4$N)]$_3$ (**3**) (Scheme 1), which was isolated as a yellow powder in 91% yield. Compound **3** can be accessed directly from the reaction of Ru($\eta^4$-C$_8$H$_{12}$)($\eta^6$-C$_8$H$_{10}$) with 3.2 equiv of the ligand at 60 °C. Compound **3** can also be achieved from **2** by heating at 50 °C with a slight excess of an equivalent of the ligand. The $^1$H NMR integration ratios of **3** indicate that there are three SiMe$_2$ groups in comparison to a single hydride at $\delta = -14.27$ ppm. The hydride singlet has $^{29}$Si satellites and a coupling constant $J_{SiHapp} = 9.0$ Hz. A single silicon singlet at $\delta = 64.28$ ppm is observed in the (H,Si)-HMQC NMR spectrum at room temperature indicating that the SiMe$_2$ groups are equivalent in solution. At 173 K, no change is observed with a single resonance, both for the $^1$H and the $^{29}$Si signals. The (H,N)-HMQC NMR spectrum has a signal at $\delta = -151.4$ ppm for the coordinating pyridinic nitrogen and one at $\delta = -284.8$ ppm for the amino nitrogen. The X-ray structure of **3** shown in Figure 3 confirms the coordination of three silazane moieties

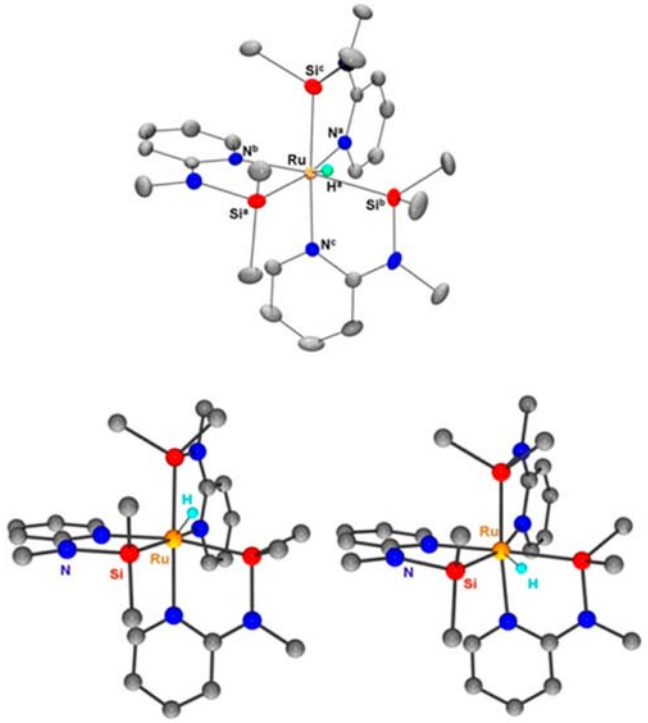


**Figure 3.** Top: X-ray molecular structure of **3** (ellipsoids are shown at 50% probability with hydrogen atoms represented by green spheres or excluded for clarity). Bottom: Optimized DFT strutures of **3a** (left) and **3b** (right).

together with the single hydride. The geometric parameters of **3** obtained by X-ray and DFT calculations are listed in Table 3. Complex **3**, similarly to the previously reported complex Ru(H)[$\kappa$-Si,N-(SiMe$_2$)N(C$_5$H$_4$N)(SiMe$_2$H)]$_3$ (**4**),[4] incorporates three bidentate pyridylsilazane ligands and a hydride in the coordination sphere of ruthenium. However, **4** was found to be symmetric by X-ray and neutron diffraction with the hydride ligand positioned in the middle of three symmetry-related silicon atoms (three equal Si−H distances: 2.120(9) Å by X-ray, 2.154(8) Å by neutron, and 2.162 Å by DFT). In contrast, the X-ray structure of **3** indicates two Si−H distances shorter than the third with the corresponding Ru−Si distances longer as one would expect if there were two Si−H interactions stronger than the other. The N−Ru−Si angles are also unequal, further reflecting the lower degree of symmetry of the molecule. A DFT study found that the two structures, **3a** and **3b**, the former symmetric and the latter less regular, are degenerate.


dx.doi.org/10.1021/ic302682f | Inorg. Chem. 2013, 52, 2654−2661

**Table 3. Comparison between Selected Bond Distances (Å) and Angles (deg) for the Experimental and Calculated Structures of 3**

| | X-ray | DFT | |
|---|---|---|---|
| | 3 | 3b | 3a |
| $Ru-H_a$ | 1.42(3) | 1.586 | 1.558 |
| $Si_a-H_a$ | 1.97(3) | 1.891 | 2.16 |
| $Si_b-H_a$ | 2.00(3) | 2.042 | |
| $Si_c-H_a$ | 2.33(3) | 2.929 | |
| $Ru-Si_a$ | 2.3213(5) | 2.351 | 2.34 |
| $Ru-Si_b$ | 2.3264(5) | 2.359 | |
| $Ru-Si_c$ | 2.3117(5) | 2.33 | |
| $N_a-Ru-Si_a$ | 168.93(4) | 163.90 | 169.75 |
| $N_b-Ru-Si_b$ | 170.46(4) | 168.39 | |
| $N_c-Ru-Si_c$ | 172.12(4) | 172.67 | |

Geometrical parameters are given in Table 3. Thus, we note that, in a $Ru-H-Si_3$ system, it is equally energetically favorable for there to be two strong silicon hydrogen interactions as for there to be three equivalent yet slightly weaker silicon hydrogen interactions. The potential energy surface is very flat, coherent with the description of weak Si–H interactions and a highly delocalized hydride.[11] The experimental structure geometry is intermediate between those of the two lowest energy calculated geometries **3a** and **3b**. In solution, NMR data are consistent with a symmetrical environment.

The $Ru-H-Si_2$ interaction of the dimeric species **2** is interesting in relation to the $Ru-H-Si_3$ system of **3**. The two short Si–H distances of **3** are identical, 1.97(3) and 2.00(3) Å, and the same as the Si–H distance in **2**, 1.96(2) Å reaffirming that it is favorable for the hydride to be located equidistant between two silicon atoms even in the presence of a third. In solution, however, the silicon hydrogen coupling constants of **2**, 28.0 Hz, and **3**, 9.0 Hz, are significantly different suggesting a weaker Si–H interaction in **3**.[9] However, care must be taken when using these coupling constants as indicators of the strength of the interaction between the atoms because the apparent $J_{SiHapp}$ is most likely a combination of $^1J_{SiH}$, always negative, with $^2J_{SiH}$, sometimes negative, and it is difficult to meaningfully separate the contributions made to $J_{SiHapp}$ by the different orders.[5a,10]

**Protonation of 3. Single Crystal Neutron Diffraction Structure of 5.** The reaction of **3** with an equivalent of $[H(OEt_2)_2]^+[(3,5\text{-}(CF_3)_2C_6H_3)_4B]^-$ gave $[RuH\{(\eta^2\text{-}HSiMe_2)N(Me)\kappa\text{-}N\text{-}(C_5H_4N)\}\{\kappa\text{-}Si,N\text{-}(SiMe_2)N(Me)(C_5H_4N)\}_2]^+[BAr^F{}_4]^-$ (**5**) ($BAr^F{}_4$ = $B(3,5\text{-}(CF_3)_2C_6H_3)_4$), which was isolated as a brown powder in 76% yield (Scheme 2). In this case, the $^1H$ NMR integration ratios show that there are two hydrides at $\delta = -15.23$ ppm in comparison to the three $SiMe_2$ groups. The hydride singlet has $^{29}Si$ satellites and a coupling constant of $J_{SiHapp}$ = 17.6 Hz. The (H,Si)-HMQC NMR spectrum of **5** at 298 K has a signal at $\delta$ = 50.8 ppm, and again no decoalescence could be observed at 173 K, both for $^1H$ and $^{29}Si$ NMR. The (H,N)-HMQC NMR spectrum has a signal at $\delta = -168.2$ ppm for the coordinating pyridinic nitrogen and a signal at $\delta = -290.2$ ppm for the amino nitrogen. The molecular structure of **5** was obtained by X-ray and neutron diffraction (Figure 4) enabling us to compare the two sets of structural parameters and to assess the importance of the contribution made by DFT calculations to the reliable description of metal–hydride compounds in general, bearing in mind that only five neutron studies of M–H–Si systems have been reported.[12] Table 4 displays selected geometrical parameters of **5** determined by X-ray and neutron diffraction and by DFT calculations.

**Scheme 2. Reversible Protonation of 3 Leading to 5**

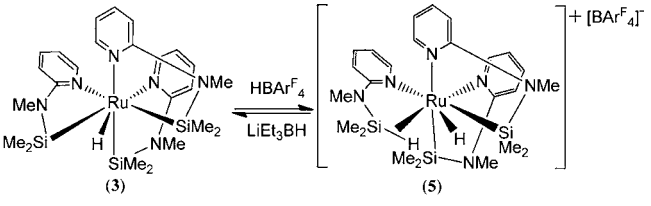


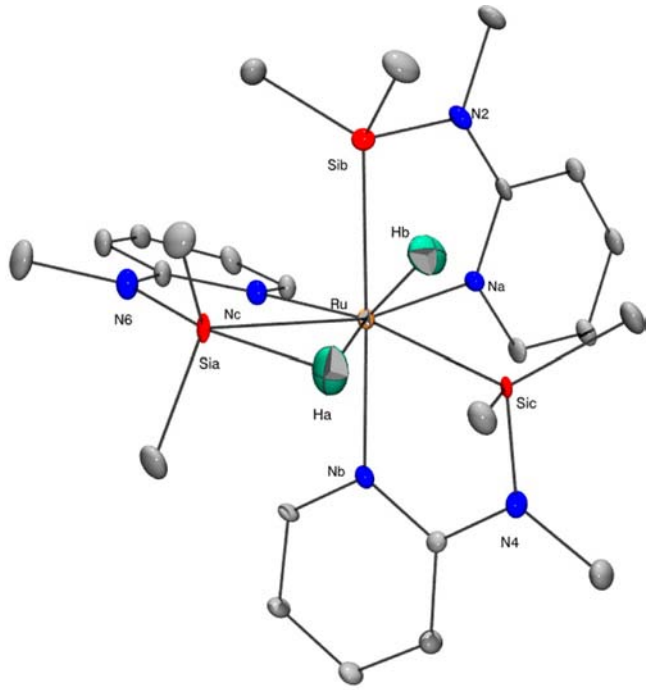


**Figure 4.** Neutron molecular structure of **5** (ellipsoids are shown at 50% probability with hydrogen atoms represented by green spheres and other hydrogens excluded for clarity.).

**Table 4. Comparison between Selected Distances (Å) and Angles (deg) for the X-ray, Neutron, and Calculated Structures of 5**

| | X-ray | Neutron | DFT |
|---|---|---|---|
| $Ru-H_a$ | 1.55(5) | 1.600(8) | 1.596 |
| $Ru-H_b$ | 1.47(4) | 1.587(7) | 1.579 |
| $Ru-Si_a$ | 2.4560(9) | 2.459(6) | 2.472 |
| $Ru-Si_b$ | 2.4105(9) | 2.408(6) | 2.431 |
| $Ru-Si_c$ | 2.3941(9) | 2.400(6) | 2.414 |
| $Si_a-H_a$ | 1.62(4) | 1.74(1) | 1.750 |
| $Si_b-H_a$ | 3.20(5) | 3.28(1) | 3.300 |
| $Si_c-H_a$ | 2.37(5) | 2.29(1) | 2.282 |
| $Si_a-H_b$ | 3.07(4) | 3.057(9) | 3.103 |
| $Si_b-H_b$ | 2.03(4) | 1.95(1) | 1.921 |
| $Si_c-H_b$ | 1.89(4) | 2.00(1) | 2.060 |
| $N_a-Ru-Si_a$ | 162.58(7) | 162.8(2) | 163.07 |
| $N_b-Ru-Si_b$ | 169.94(7) | 169.9(2) | 169.99 |
| $N_c-Ru-Si_c$ | 164.06(7) | 164.2(2) | 164.73 |


dx.doi.org/10.1021/ic302682f | Inorg. Chem. 2013, 52, 2654–2661

The Si−H neutron diffraction distances allow the formulation of **5** with an $\eta^2$-Si−H interaction (Sia−Ha = 1.74(1) Å) together with two secondary interactions between the second hydride and the remaining two silicon atoms (Sib−Hb = 1.95(1) and Sic−Hb = 2.00(1) Å). This is consistent with the differences in Ru−Si bond lengths, the longest one for the silicon involved in the $\eta^2$-Si−H bonding (Ru−$Si_a$ = 2.459 (6) Å compared to Ru−$Si_b$ = 2.408 (6) Å and Ru−$Si_c$ = 2.400 (6) Å). There is no interaction between the two hydride atoms as indicated by an interhydride distance of 1.98(2) Å and the $T_{1\ min}$ value of 620 ms at 183 K and 500 MHz, both parameters being too long to postulate a dihydrogen complex.[13] Interestingly, the reaction of **5** with a slight excess of $LiEt_3BH$ in THF regenerated **3**.

## CONCLUSION

The family of complexes presented here demonstrates the versatility in the nature of Ru−H−Si interactions that can be achieved from the reactivity of pyridine-2-amino(methyl)-dimethylsilane. The combination of two labile alkenyl ligands with the silazane in the coordination sphere of **1** endows it with great potential as a precursor to other ruthenium−silazane complexes. Accordingly, it has been possible to modulate the number of silazane ligands coordinated to ruthenium by control over stoichiometry and reaction conditions enabling useful comparisons to be drawn within a series of related complexes displaying multicenter interactions. Fine tuning of the coordination sphere of the metal has been well illustrated by the reversible protonation reaction. Studies of the effect of N-substituent modification of silazane ligands will continue with the aim of creating a series of compounds with varying basicity and electrochemical properties.

Structural studies are essential for the identification of $\eta^2$-complexes and the establishment of secondary interactions. Si−H bond distances are useful parameters with the upper limit for an $\eta^2$-Si−H bond being 1.90 Å whereas the range for SISHA is 1.90−2.40 Å. However, the location of hydrogen atoms by X-ray diffraction is subject to systematic errors that lead to an underestimate of any distance involving a hydrogen. Consequently, DFT calculations are often used, and our study confirms that DFT structural parameters are in close agreement to those obtained by neutron diffraction, a technique able to irrefutably locate hydrogen atoms.[14] It is noteworthy that the neutron structure of **5** allows unambiguous characterization of $\eta^2$-Si−H and SISHA bonds with different Si−H distances at the same metal center (1.74(1) Å for $\eta^2$-Si−H and 1.96(1)−2.29(1) Å for SISHA).

Finally, there are a few published examples of the interaction of two silicon atoms with a single hydrogen. Müller and co-workers reported the structural characterization of a disilyl cation with a bridging hydrogen and naphthyl backbone.[15] The disilyl cation $^{29}$Si NMR resonance at $\delta$ = 54.4 ppm is interesting to compare with the values of **2** ($\delta$ = 51.5 ppm) and **5** ($\delta$ = 50.8 ppm) suggesting that the electronic environment of the silicon atoms in these three compounds is similar. In addition, the experimental molecular structure of the disilyl cation is asymmetric with Si−H bond distances elongated (1.583(5) and 1.677(4) Å), in relation to a classical Si−H bond (1.481(5) Å).[4] A further example of the hydride-bridged silicon motif is provided by Reed and co-workers who have structurally characterized $[Me_3Si{-}H{-}SiMe_3][CHB_{11}Cl_{11}]$, a moiety with statistically identical Si−H distances (1.60(2) and 1.62(2) Å).[16] Multicenter bonding is an often encountered feature of silicon chemistry, one that can be expressed in the absence or presence of a transition metal.

## EXPERIMENTAL SECTION

**General Methods.** Manipulations were carried out following standard Schlenk line and glovebox techniques, with $O_2$ < 1 ppm, and Ar as the inert gas. Solvents were dried using a MBraun SPS column. Deuterated solvents were freeze−pump−thaw degassed and stored under Ar and over 4 Å molecular sieves. THF-$d_8$ was dried over sodium. $Ru(\eta^4\text{-}C_8H_{12})(\eta^6\text{-}C_8H_{10})$[17] and $[H(OEt_2)_2]^+[[3,5\text{-}(CF_3)_2C_6H_3]_4B]^-$[18] were prepared by previously published methods. Unless otherwise indicated, commercially available reagents were used as supplied and for the most part were purchased from Aldrich or AlfaAesar. NMR spectra were collected on several machines; a Bruker 500 MHz Avance, a Bruker 400 MHz Avance, a Bruker 300 MHz Avance, and a Bruker 300 MHz DPX. Chemical shifts are given in units of ppm, with coupling constants in Hz. Mass spectroscopy was carried out using a TSQ 7000 Thermo Electron mass spectrometer. Infrared spectroscopy was carried out using a Perkin-Elmer 1725 spectrometer for nujol mulls pressed between KBr disks and a Bruker Alpha P spectrometer for ATR measurements. Microanalyses were performed at the Laboratoire de Chimie de Coordination on a Perkin-Elmer 2400 Series II analyzer.

**Synthesis of Pyridine-2-amino(methyl)dimethylsilane.** 2-(Methylamino)-pyridine (4.00 g, 37.0 mmol) was dissolved in $Et_2O$ (80 mL) and cooled to −35 °C before n-BuLi (14.8 mL, 2.5 M in hexane, 37.0 mmol) was added dropwise. After 1 h of stirring at −35 °C, an $Et_2O$ solution (10 mL) of $HSiMe_2Cl$ (4.02 mL, 37.0 mmol) was added to the yellow suspension giving rise to the formation of a white precipitate. A yellow solution was obtained after filtration through Celite and the solvent evaporated. The resulting yellow oil was purified by trap-to-trap distillation at 75 °C to afford a colorless oil (4.97 g, 81%). $^1$H NMR (400.12 MHz, $C_6D_6$, 298 K): 8.20 (dd, 1 H, Pyr, $^3J_{HH}$ = 4.8, $^4J_{HH}$ = 1.1), 7.26 (ddd, 1 H, Pyr, $^3J_{HH}$ = 8.8, $^3J_{HH}$ = 7.2, $^4J_{HH}$ = 2.0), 6.47 (dd, 1 H, Pyr, $^3J_{HH}$ = 7.0, $^3J_{HH}$ = 5.0), 6.28 (d, 1 H, Pyr, $^3J_{HH}$ = 8.4), 5.02 (sept, 1 H, SiH, $^3J_{HH}$ = 3.6, $^1J_{SiH}$ = 197.1), 2.16 (s, 3H, NMe), 0.61 (dd, 6 H, SiMe, $^2J_{SiH}$ = 10.2, $^3J_{HH}$ = 3.1). $^{13}$C{$^1$H} NMR (100.62 MHz, $C_6D_6$, 298 K): 161.74 (Pyr quaternary), 147.33 (Pyr), 137.44 (Pyr), 112.88 (Pyr), 105.63 (Pyr), 33.01(NMe), −0.89 (SiMe). $^{15}$N NMR (40.55 MHz, $C_6D_6$, 298 K): −104.4 (Pyr), −312.2 (NMe). $^{29}$Si DEPT NMR (79.50 MHz, $C_6D_6$, 298 K): −4.14 (s). IR (Nujol mull, cm$^{-1}$) 2115 weak ($\nu_{Si-H}$). Positive CI-MS: $m/z$ 167 $[M + 1]^+$ (100%). Negative CI-MS: $m/z$ 107 $[C_6H_7N_2]^-$ (100%).

**Synthesis of Ru[κ-Si,N-(SiMe$_2$)N(Me)(C$_5$H$_4$N)]($\eta^4$-C$_8$H$_{12}$)($\eta^3$-C$_8$H$_{11}$) (1).** A pentane solution (1 mL) of pyridine-2-amino(methyl)-dimethylsilane (0.240 g, 1.425 mmol) was added to a pentane solution (6 mL) of $Ru(\eta^4\text{-}C_8H_{12})(\eta^6\text{-}C_8H_{10})$ (0.300 g, 0.951 mmol) at room temperature and the solution stirred for 10 min after which time the formation of a yellow precipitate was observed. The suspension was allowed to stir for 15 h. The precipitate was isolated by filtration and rinsed with pentane (3 mL) to afford the pure product, a lemon yellow powder (0.370 g, 81%). Yellow crystals suitable for X-ray analysis were grown from a pentane solution. $^1$H NMR (500.33 MHz, $C_6D_6$, 301 K): (see Figure S1 for (H,C)-HSQC NMR spectrum; see below for atom numeration) 7.58 (dd, 1 H, **H3** Pyr, $^3J_{HH}$ = 6.0, $^4J_{HH}$ = 1.5), 6.84 (ddd, 1 H, **H5** Pyr, $^3J_{HH}$ = 9.0, $^3J_{HH}$ = 7.0, $^4J_{HH}$ = 2.0), 6.71 (dd, 1 H, **H20** $\eta^3$-$C_8H_{11}$, $^3J_{HH}$ = 10.5, $^3J_{HH}$ = 2.5), 5.92 (dd, 1 H, **H4** Pyr, $^3J_{HH}$ = 6.0, $^4J_{HH}$ = 1.0), 5.78 (d, 1 H, **H6** Pyr, $^3J_{HH}$ = 8.5), 5.45 (ddd, 1 H, **H21** $\eta^3$-$C_8H_{11}$, $^3J_{HH}$ = 10.0, $^3J_{HH}$ = 8.5, $^3J_{HH}$ = 1.0), 5.30 (dd, 1 H, **H19** $\eta^3$-$C_8H_{11}$, $^3J_{HH}$ = 8.5, $^3J_{HH}$ = 2.0), 3.36 (dddd, 1H, **H11** $\eta^4$-$C_8H_{12}$, $^2J_{HH}$ = 13.7, $^3J_{HH}$ = 10.8, $^3J_{HH}$ = 10.8, $^3J_{HH}$ = 5.4), 3.06 (dd, 1 H, **H10** $\eta^4$-$C_8H_{12}$, $^3J_{HH}$ = 9.0, $^3J_{HH}$ = 5.5), 3.00 (m, 1 H, **H22** $\eta^3$-$C_8H_{11}$), 2.98 (m, 1 H, **H18** $\eta^3$-$C_8H_{11}$), 2.97 (m, 1 H, **H15** $\eta^4$-$C_8H_{12}$), 2.91 (dd, 1 H, **H11** $\eta^4$-$C_8H_{12}$, $^2J_{HH}$ = 14.5, $^3J_{HH}$ = 9.0), 2.77 (dd, 1 H, **H9** $\eta^4$-$C_8H_{12}$, $^3J_{HH}$ = 8.5, $^3J_{HH}$ = 4.0), 2.68 (m, 1 H, **H17** $\eta^3$-$C_8H_{11}$), 2.66 (m, 1 H, **H14** $\eta^4$-$C_8H_{12}$), 2.62 (s, 3 H, NMe), 2.44 (dd, 1 H, **H15** $\eta^4$-$C_8H_{12}$, $^2J_{HH}$ = 14.0, $^3J_{HH}$ = 8.5), 2.33 (m, 1 H, **H16** $\eta^4$-$C_8H_{12}$), 2.27 (m, 1 H, **H12** $\eta^4$-$C_8H_{12}$), 2.21 (m, 1 H, **H22** $\eta^3$-$C_8H_{11}$), 1.74 (dddd, 1 H, **H16** $\eta^4$-$C_8H_{12}$, $^2J_{HH}$ = 13.3, $^3J_{HH}$ = 8.8, $^3J_{HH}$ = 8.8, $^3J_{HH}$ = 4.3), 1.52 (m, 1 H,


dx.doi.org/10.1021/ic302682f | Inorg. Chem. 2013, 52, 2654−2661

**H24** $\eta^3$-$C_8H_{11}$), 1.50 (m, 1 H, **H12** $\eta^4$-$C_8H_{12}$), 1.47 (m, 1 H, **H13** $\eta^4$-$C_8H_{12}$), 1.43 (m, 1 H, **H23** $\eta^3$-$C_8H_{11}$), 1.30 (ddddd, 1 H, **H23** $\eta^3$-$C_8H_{11}$, $^2J_{HH}$ = 12.7, $^3J_{HH}$ = 11.2, $^3J_{HH}$ = 5.6, $^3J_{HH}$ = 5.6, $^3J_{HH}$ = 2.1), 1.06 (s, 3 H, SiMe), 0.88 (s, 3 H, SiMe), −0.02 (dddd, 1 H, **H24** $\eta^3$-$C_8H_{11}$, $^2J_{HH}$ = 18.7, $^3J_{HH}$ = 13.8, $^3J_{HH}$ = 11.0, $^3J_{HH}$ = 5.2). $^{13}C\{^1H\}$ NMR (125.81 MHz, $C_6D_6$, 301 K): 163.73 (**C7** Pyr), 149.80 (**C3** Pyr), 137.07 (**C20** $\eta^3$-$C_8H_{11}$), 136.46 (**C5** Pyr),123.89 (**C21** $\eta^3$-$C_8H_{11}$), 111.96 (**C4** Pyr), 106.85 (**C18** $\eta^3$-$C_8H_{11}$), 105.67 (**C6** Pyr), 74.32 (**C13** $\eta^4$-$C_8H_{12}$), 70.17 (**C9** $\eta^4$-$C_8H_{12}$), 70.03 (**C19** $\eta^3$-$C_8H_{11}$), 69.70 (**C10** $\eta^4$-$C_8H_{12}$), 67.76 (**C14** $\eta^4$-$C_8H_{12}$), 58.55 (**C17** $\eta^3$-$C_8H_{11}$), 37.18 (**C15** $\eta^4$-$C_8H_{12}$), 35.68 (**C11** $\eta^4$-$C_8H_{12}$), 31.87 (NMe), 28.13 (**C16** $\eta^4$-$C_8H_{12}$), 27.05 (**C12** $\eta^4$-$C_8H_{12}$), 26.23 (**C22** $\eta^3$-$C_8H_{11}$), 25.45 (**C23** $\eta^3$-$C_8H_{11}$), 23.56 (**C24** $\eta^3$-$C_8H_{11}$), 6.99 (SiMe), 3.22 (SiMe). $^{15}N$ HMQC NMR (50.7 MHz, $C_6D_6$, 301 K): −168.7 (Pyr), −282.9 (NMe). $^{29}Si$ HMQC NMR (99.4 MHz, $C_6D_6$, 301 K): 81.0. Anal. Calcd for $C_{24}H_{56}N_2SiRu$: C, 59.84; H, 7.53; N, 5.82. Found: C, 59.72; H, 7.67; N, 5.70.

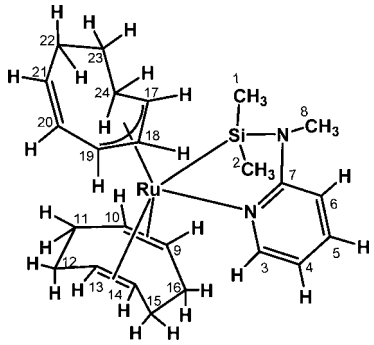


**Synthesis of $Ru_2(\mu\text{-}H)_2(H)_2[\kappa\text{-}Si,N\text{-}(SiMe_2)N(Me)(C_5H_4N)]_4$ (2).** A THF solution (1 mL) of pyridine-2-amino(methyl)dimethylsilane (17.0 mg, 0.104 mmol) was combined with a THF solution (2 mL) of $Ru[\kappa\text{-}Si,N\text{-}(SiMe_2)N(Me)(C_5H_4N)](\eta^4\text{-}C_8H_{12})(\eta^3\text{-}C_8H_{11})$ (50.0 g, 0.104 mmol). The solution was stirred for 3 h under a pressure of $H_2$ (3 bar) after which time the solvent was evaporated and the resultant dark red solid dried under vacuum. The solid was washed with pentane (2 × 3 mL), and isolation of the pentane insoluble species afforded the pure compound, a red powder (20 mg, 22%). Red crystals suitable for X-ray analysis were grown from a $C_6D_6$ solution. $^1H$ NMR (400.13 MHz, $C_6D_6$, 298 K): 8.75 (dd, 4 H, Pyr, $^3J_{HH}$ = 5.9, $^4J_{HH}$ = 1.7), 6.70 (ddd, 4 H, Pyr, $^3J_{HH}$ = 8.7, $^3J_{HH}$ = 7.1, $^4J_{HH}$ = 1.9), 5.82 (d, 4 H, Pyr, $^3J_{HH}$ = 8.3), 5.49 (dd, 4 H, Pyr, $^3J_{HH}$ = 6.4, $^4J_{HH}$ = 1.2), 2.77 (s, 12 H, NMe), 1.34 (s, 12 H, SiMe), 0.57 (s, 12 H, SiMe), −1.32 (t, 2 H, $\mu$-H, $^2J_{HH}$ = 7.1), −9.66 (t, 2 H, $H_{terminal}$, $^2J_{HH}$ = 7.2, $J_{HSiapp}$ = 28.0). $^1H$ NMR (500.32 MHz, THF-$d_8$, 193 K): no decoalesence, −1.72 (t, 2 H, $\mu$-H, $^2J_{HH}$ = 13), −10.20 (t, 2 H, $H_{terminal}$, $^2J_{HH}$ = 14, $J_{HSiapp}$ = 28.0). $^{13}C\{^1H\}$ NMR (100.61 MHz, $C_6D_6$, 298 K): 166.16 (Pyr quaternary) 157.55 (Pyr), 133.98 (Pyr), 110.02 (Pyr), 104.87 (Pyr), 31.74 (NMe), 9.94 (SiMe), 9.36 (SiMe). $^{15}N$ HMQC NMR (40.55 MHz, $C_6D_6$, 298 K): −171.9 (Pyr), −287.1 (NMe). $^{29}Si$ HMQC NMR (79.49 MHz, $C_6D_6$, 298 K): 51.5. $^{29}Si$ HMQC NMR (99.40, MHz, THF-$d_8$, 193 K): 50.0. IR ATR measured ($cm^{-1}$) 2068 ($\upsilon_{Ru-H}$, weak). IR DFT and corrected with a coefficient factor of 0.96 ($cm^{-1}$) 2040 ($\upsilon_{Ru-H}$). Anal. Calcd for $C_{32}H_{56}N_8Si_4Ru$: C, 44.31; H, 6.51; N, 12.99. Found: C, 44.24; H, 6.75; N, 12.80.

**Synthesis of $Ru(H)[\kappa\text{-}Si,N\text{-}(SiMe_2)N(Me)(C_5H_4N)]_3$ (3).** A THF solution (2 mL) of pyridine-2-amino(methyl)dimethylsilane (0.841 g, 5.06 mmol) was added to a THF solution (15 mL) of $Ru[\kappa\text{-}Si,N\text{-}(SiMe_2)N(Me)(C_5H_4N)](\eta^4\text{-}C_8H_{12})(\eta^3\text{-}C_8H_{11})$ (0.950 g, 2.024 mmol). The resulting yellow solution was stirred for 3 h at 60 °C. After cooling to room temperature, the solvent was evaporated to leave a yellow solid that was dried under vacuum for 0.75 h and washed with cold pentane (2 × 4 mL, −20 °C) to afford the pure product, a yellow powder (0.991 g, 91%). Yellow crystals suitable for X-ray analysis were grown from a pentane solution. $^1H$ NMR (400.13 MHz, $C_6D_6$, 298 K): 7.58 (dd, 3 H, Pyr, $^3J_{HH}$ = 5.7, $^4J_{HH}$ = 1.5), 7.09 (ddd, 3 H, Pyr, $^3J_{HH}$ = 8.8, $^3J_{HH}$ = 6.9, $^4J_{HH}$ = 1.9), 6.23 (d, 3 H, Pyr, $^3J_{HH}$ = 8.7), 6.03 (ddd, 3 H, Pyr, $^3J_{HH}$ = 6.9, $^3J_{HH}$ = 5.8, $^4J_{HH}$ = 1.2), 2.70 (s, 9 H, NMe), 0. 87 (s, 9 H, SiMe), 0.14 (s, 9 H, SiMe), −14.27 (s, 1 H, Ru−H, $J_{SiHapp}$ = 9.0). $^1H$ NMR (500.32 MHz, THF-$d_8$, 298 K): 7.45 (ddd, 3 H, Pyr, $^3J_{HH}$ = 8.7, $^3J_{HH}$ = 8.6, $^4J_{HH}$ = 5.1), 7.19 (dd, 3 H, Pyr, $^3J_{HH}$ = 5.7, $^4J_{HH}$ = 1.6), 6.51 (dd, 3 H, Pyr, $^3J_{HH}$ = 8.6, $^4J_{HH}$ = 1), 6.23 (d, 3 H, Pyr, $^3J_{HH}$ = 5.9), 2.82 (s, 9 H, NMe), 0.40 (s, 9 H, SiMe), −0.33 (s, 9 H, SiMe), −14.69 (s, 1 H, Ru−H, $J_{SiHapp}$ = 9). $^{13}C\{^1H\}$ NMR (100.61 MHz, $C_6D_6$, 298 K): 165.00 (Pyr quaternary), 148.64 (Pyr), 136.69 (Pyr), 110.96 (Pyr), 107.04 (Pyr), 31.79 (NMe), 9.00 (SiMe), 3.24 (SiMe). $^{15}N$ HMQC (40.55 MHz, THF-$d_8$, 298 K): −151.4 (Pyr), −284.8 (NMe). $^{29}Si$ DEPT NMR (79.50 MHz, $C_6D_6$, 298 K): 64.28.

**Table 5. Selected X-ray Data Collection and Refinement Parameters for 1, 2, 3, and 5**

| | 1 | 2 | 3 | 5 |
|---|---|---|---|---|
| formula | $C_{24}H_{36}N_2RuSi$ | $C_{32}H_{56}N_8Ru_2Si_4$ | $C_{24}H_{40}N_6RuSi_3$ | $C_{32}H_{12}BF_{24}$, $C_{24}$ $H_{41}N_6RuSi_3$ |
| fw | 481.71 | 867.35 | 597.96 | 1462.19 |
| cryst syst | monoclinic | tetragonal | orthorhombic | monoclinic |
| space group | $P2_1/n$ | $P4_22_12$ | $P2_12_12_1$ | $Pn$ |
| $a$ (Å) | 14.2470(10) | 12.5360(2) | 9.6790(6) | 13.9065(3) |
| $b$ (Å) | 16.0730(10) | 12.5360(2) | 16.0690(8) | 12.1742(3) |
| $c$ (Å) | 19.4300(10) | 12.8809(2) | 36.6520(18) | 18.3076(4) |
| $\alpha$ (deg) | 90 | 90 | 90 | 90 |
| $\beta$ (deg) | 101.564(10) | 90 | 90 | 94.385(2) |
| $\gamma$ (deg) | 90 | 90 | 90 | 90 |
| $V$ (Å$^3$) | 4359.0(5) | 2024.25(6) | 5700.6(5) | 3090.41(12) |
| $Z$ | 8 | 2 | 8 | 2 |
| $T$ (K) | 100(2) | 100(2) | 100(2) | 100(2) |
| $\rho_{calcd}$ (g cm$^{-3}$) | 1.468 | 1.423 | 1.393 | 1.571 |
| $\mu$(mm$^{-1}$) | 0.787 | 0.897 | 0.700 | 0.428 |
| no. rflns collctd | 72 183 | 11 004 | 123 481 | 61 811 |
| no. indep rflns | 17 633 | 2076 | 11 635 | 12 620 |
| no. params | 511 | 113 | 639 | 837 |
| $R_{int}$ | 0.0778 | 0.0244 | 0.0288 | 0.0429 |
| R1/wR2, $I \geq 2\sigma(I)$ | 0.0424/0.0679 | 0.0156/0.0352 | 0.0161/0.0393 | 0.0345/0.0809 |
| R1/wR2, all data | 0.1080/0.0816 | 0.0188/0.0356 | 0.0169/0.0398 | 0.0399/0.0854 |
| GOF | 0.986 | 0.992 | 1.110 | 1.041 |


dx.doi.org/10.1021/ic302682f | Inorg. Chem. 2013, 52, 2654−2661

$^{29}$Si HMQC NMR (99.40, MHz, THF-$d_8$, 173 K): 63.0. Anal. Calcd for $C_{24}H_{40}N_6RuSi_3$: C, 48.21; H, 6.74; N, 14.06. Found: C, 48.21: H, 6.93; N, 13.97.

**Synthesis of {Ru[($\eta^2$-H−SiMe$_2$)N(Me)$\kappa$-N-(C$_5$H$_4$N)[$\kappa$-Si,N-(SiMe$_2$)N(Me)(C$_5$H$_4$N)]}$^+${[3,5-(CF$_3$)$_2$C$_6$H$_3$]$_4$B}$^-$ (5).** A $CH_2Cl_2$ solution (2 mL) of $[H(OEt_2)_2]^+[[3,5\text{-}(CF_3)_2C_6H_3]_4B]^-$ (0.177 g, 0.167 mmol) was added to a $CH_2Cl_2$ solution (3 mL) of **3** (0.100 g, 0.167 mmol). The resulting brown solution was stirred for 1 h at 20 °C after which time the solvent was evaporated to leave a brown solid that was washed with pentane (4 × 2 mL) to afford the pure product, a light brown powder (0.186 g, 76%). Green crystals suitable for X-ray diffraction were grown from a saturated $CH_2Cl_2$ solution at −37 °C. $^1$H NMR (400.13 MHz, $CD_2Cl_2$, 298 K): 7.76 (s, 12 H, BAr$^F$), 7.70 (t, 3 H, Pyr, $^3J_{HH}$ = 8.4, $^4J_{HH}$ = 1.4), 7.60 (s, 6 H, BAr$^F$), 6.89 (dd, 3 H, Pyr, $^3J_{HH}$ = 5.9), 6.78 (d, 3 H, Pyr, $^3J_{HH}$ = 8.7), 6.53 (t, 3 H, Pyr, $^3J_{HH}$ = 6.4), 2.96 (s, 9 H, NMe), 0.63 (s, 9 H, SiMe), −0.03 (s, 9 H, SiMe), −15.23 (s, 2 H, Ru−H, $J_{SiHapp}$ = 17.6). $^1$H NMR (500.32 MHz, THF-$d_8$, 173 K): no decoalescence, −15.21(s, 2 H, Ru−H, $J_{SiHapp}$ = 15.0). $^{13}$C{$^1$H} NMR (100.61 MHz, $CD_2Cl_2$, 298 K): 163.74 (Pyr quaternary), 161.72 (q, $^1J_{BC}$ = 49.7 BAr$^F$, i-C), 147.34 (Pyr), 140.21 (Pyr), 134.77 (BAr$^F$, o-C), 128.83 (q, $^2J_{CF}$ = 31.2, BAr$^F$, m-C), 123.22 (q, $CF_3$ $^1J_{CF}$ = 272.1), 117.45 (BAr$^F$, p-C), 114.36 (Pyr), 109.69 (Pyr), 32.17 (NMe), 8.04 (SiMe), 2.64 (SiMe). $^{29}$Si HMQC NMR (79.50, MHz, $CD_2Cl_2$, 298 K): 50.76. $^{29}$Si HMQC NMR (99.40, MHz, THF-$d_8$, 173 K): 50.60. $^{11}$B{$^1$H} NMR (160.53 MHz, THF-$d_8$, 301.1 K): −6.50. $^{15}$N HMQC NMR (40.55 MHz, $CD_2Cl_2$, 298 K): −168.2, −290.2. $T_{1\ min}$ of the hydride signal in THF-$d_8$ at 500.32 MHz and 183 K is 0.62 s. Anal. Calcd for $C_{56}H_{53}N_6BF_{24}Si_3Ru$: C, 46.01; H, 3.65; N, 5.75. Found: C, 45.65: H, 3.25; N, 5.97.

**Reaction of Complex 5 with Li$^+$[HB(C$_2$H$_5$)$_3$]$^-$.** $Li^+[HB(C_2H_5)_3]^-$ (72.8 $\mu$L of a 1 M solution in THF, 0.069 mmol) was added to a brown solution of **5** (0.100 g, 0.053 mmol) in THF (6 mL). The homogeneous brown solution was stirred for 2.5 h before the solvent was evaporated and the brown solid dried under vacuum for 2.5 h. The NMR spectrum of the resulting species in THF-$d_8$ was compared to the spectrum of **3** in THF-$d_8$ to confirm the regeneration of **3** from **5**.

**Computational Details.** DFT calculations employing the B3PW91[19] functional were performed with the GAUSSIAN03 series of programs.[20] The ruthenium and silicon atoms were represented by the relativistic effective core potential (RECP) from the Stuttgart group and their associated basis set,[21] augmented by polarization functions ($\alpha_f$ = 1.235, Ru; $\alpha_d$ = 0.284, Si).[22] The remaining atoms (C, N, H) were represented by 6-31G(d,p) basis sets.[23] Full optimizations of geometry without any constraint were performed. Calculations of harmonic vibrational frequencies were performed to determine the nature of each extremum. Cartesian coordinates in Å for the calculated geometries. The contributions to the Gibbs free energy were taken at $T$ = 298 K and with $P$ = 1 atm within the harmonic oscillator and rigid rotator approximations.

**X-ray Data.** Important crystallographic data are given in Table 5; the experimental procedure and relevant data are in the Supporting Information as CIF data (also deposited at the CCDC: **1**, CCDC 905933, **2**, CCDC 905932, **3**, CCDC 905930, and **5**, CCDC 905931).

**Neutron Data.** A prismatic crystal, with a volume of ca. 0.82 mm$^3$, was mounted in an inert Ar atmosphere inside a thin-walled quartz cryorefrigerator.[24] The sample was mounted on a Displex cryorefrigerator on the ILL thermal-beam diffractometer D19 equipped with the new horizontally curved "banana-shaped" position-sensitive detector[25] and cooled to 20 K. The Bragg intensities were corrected for attenuation by the vanadium Displex heat-shields and analytically for the crystal absorption.

The starting structural model was based on the atomic coordinates from the X-ray structural determination, while the positions of H atoms bonded to the Ru center were found from a difference Fourier map. The structure was refined by full matrix least-squares, minimizing the function $[\sum w(F_o^2 - (1/k)F_c^2)^2]$ and using all the independent data. Anisotropic displacement parameters (ADPs) were used for all atoms, while the site occupancy factors (SOF) of the hydrides were left to refine freely in order to check that these sites were fully occupied, and then fixed at 1.00 for the final refinement cycles. Upon convergence the final Fourier difference map showed no significant features. Further crystallographic data, experimental details and geometrical parameters are given in Table 6, in the Supporting Information, and as a CIF file (also as CCDC 905934).

**Table 6. Crystal Data and Details of the Structure Refinement for the Neutron Diffraction Study of 5**

| formula | $C_{56}H_{53}$ $BF_{24}N_6$ $RuSi_3$ |
|---|---|
| mol wt | 1462.19 |
| data coll $T$, K | 20 (1)K |
| radiation | neutrons ($\lambda$ = 1.1708 (1) Å) |
| cryst syst | Monoclinic |
| space group (No.) | $Pn$ (7) |
| $a$, Å | 13.9659 (3) |
| $b$, Å | 11.9966 (4) |
| $c$, Å | 18.2189 (5) |
| $\beta$, deg | 94.011 (2) |
| $V$, Å$^3$ | 3045.0 (2) |
| $Z$ | 2 |
| $\rho_{calcd}$, g cm$^{-3}$ | 1.596 |
| $\mu$, mm$^{-1}$ | 0.183 |
| no. data collected | 27 927 |
| $\theta$ range (deg) | 4.8−61.3 |
| no. indep data | 9494 |
| no. obsd reflns ($n_o$) | 7647 |
| no. params refined ($n_v$) | 1297 |
| $R_{int}$ | 0.1253 |
| $R(F_o)$ [$I > 2\sigma(I)$][a] | 0.0617 |
| $R_w(F_o^2)$ [$I > 2\sigma(I)$][a] | 0.1197 |
| GOF[a] | 1.063 |

[a] $R_{int} = \Sigma|F_o^2 - \langle F_o^2\rangle|/\Sigma F_o^2$; $R(F_o) = \Sigma||F_o| - |F_c||/\Sigma|F_o|$; $R_w(F_o^2) = [\Sigma[w(F_o^2 - F_c^2)^2]/\Sigma[w(F_o^2)^2]]^{1/2}$; GOF = $[\Sigma[w(F_o^2 - F_c^2)^2]/(N - P)]^{1/2}$, where $N$ and $P$ are the numbers of observations and parameters, respectively.

## ■ ASSOCIATED CONTENT

### Supporting Information

(H,C) HSQC NMR spectrum of **1**. Neutron diffraction experimental and structural details for compound **5**. Coordinates of the calculated structures **1**, **2**, **3a**, **3b**, and **5**. CIF data for complexes **1**, **2**, **3**, and **5** (X-ray and neutron). This material is available free of charge via the Internet at http://pubs.acs.org.

## ■ AUTHOR INFORMATION


### Corresponding Author

*E-mail: mary.grellier@lcc-toulouse.fr (M.G.); sylviane.sabo@lcc-toulouse.fr (S.S.-E.).


### Author Contributions

The manuscript was written through contributions of all authors. All authors have given approval to the final version of the manuscript.

### Notes

The authors declare no competing financial interest.

## ■ ACKNOWLEDGMENTS


We thank the CNRS for support and Johnson Matthey plc for the generous gift of hydrated ruthenium trichloride. K.A.S. thanks the French Ministry of Research for a Ph.D. fellowship. Computer time was given by the HPC resources of CALMIP (Toulouse, France) under the allocation 2012-[P0909]. A.A. thanks MIUR (PRIN 2009) for financial support.

## REFERENCES


(1) (a) Trost, B. M.; Ball, Z. T. *J. Am. Chem. Soc.* **2003**, *125*, 30−31. (b) Zapilko, C.; Widenmeyer, M.; Nagl, I.; Estler, F.; Anwander, R.; Raudaschl-Sieber, G.; Groeger, O.; Engelhardt, G. *J. Am. Chem. Soc.* **2006**, *128*, 16266−16276. (c) Deschner, T.; Törnroos, K. W.; Anwander, R. *Inorg. Chem.* **2011**, *50*, 7217−7228. (d) Lekishvili, N.; Samakashvili, S.; Lekishvili, G. *New Silazane Monomers and Polymers: Synthesis, Properties and Application*; Nova Science Publishers, Inc.: Hauppauge, NY, 2007. (e) Colombo, P.; Mera, G.; Riedel, R.; Soraru, G. D. *J. Am. Ceram. Soc.* **2010**, *93*, 1805−1837. (f) Dai, M.; Wang, Y.; Kwon, J.; Halls, M. D.; Chabal, Y. J. *Nat. Mater.* **2009**, *8*, 825−830.

(2) (a) Dunne, J. F.; Neal, S. R.; Engelkemier, J.; Ellern, A.; Sadow, A. D. *J. Am. Chem. Soc.* **2011**, *133*, 16782−16785. (b) Meermann, C.; Gerstberger, G.; Spiegler, M.; Törnroos, K. W.; Anwander, R. *Eur. J. Inorg. Chem.* **2008**, *2008*, 2014−2023. (c) Ionescu, E.; Kleebe, H.-J.; Riedel, R. *Chem. Soc. Rev.* **2012**, *41*, 5032−5052. (d) Dargère, N.; Bounor-Legaré, V.; Boisson, F.; Cassagnau, P.; Martin, G.; Sonntag, P.; Garois, N. *J. Sol-Gel Sci. Technol.* **2012**, *62*, 389−396. (e) Brulé, E.; Gaillard, S.; Rager, M.-N. l.; Roisnel, T.; Guérineau, V.; Nolan, S. P.; Thomas, C. M. *Organometallics* **2011**, *30*, 2650−2653.

(3) Ayed, T.; Barthelat, J.-C.; Tangour, B.; Pradère, C.; Donnadieu, B.; Grellier, M.; Sabo-Etienne, S. *Organometallics* **2005**, *24*, 3824−3826.

(4) Grellier, M.; Ayed, T.; Barthelat, J.-C.; Albinati, A.; Mason, S. A.; Vendier, L.; Coppel, Y.; Sabo-Etienne, S. *J. Am. Chem. Soc.* **2009**, *131*, 7633−7640.

(5) (a) Corey, J. Y. *Chem. Rev.* **2011**, *111*, 863−1071. (b) Marciniec, B. *Coord. Chem. Rev.* **2005**, *249*, 2374−2390. (c) Corey, J. Y.; Braddock-Wilking, J. *Chem. Rev.* **1999**, *99*, 175−292. (d) Gutsulyak, D. V.; Vyboishchikov, S. F.; Nikonov, G. I. *J. Am. Chem. Soc.* **2010**, *132*, 5950−5951. (e) Gutsulyak, D. V.; van der Est, A.; Nikonov, G. I. *Angew. Chem., Int. Ed.* **2011**, *50*, 1384−1387. (f) Yang, J.; Tilley, T. D. *Angew. Chem., Int. Ed.* **2010**, *49*, 10186−10188. (g) Sadow, A. D.; Tilley, T. D. *Angew. Chem., Int. Ed.* **2003**, *42*, 803−805. (h) Khalimon, A. Y.; Simionescu, R.; Nikonov, G. I. *J. Am. Chem. Soc.* **2011**, *133*, 7033−7053.

(6) (a) Six, C.; Gabor, B.; Görls, H.; Mynott, R.; Philipps, P.; Leitner, W. *Organometallics* **1999**, *18*, 3316−3326. (b) Hermatschweiler, R.; Fernández, I.; Pregosin, P. S.; Watson, E. J.; Albinati, A.; Rizzato, S.; Veiros, L. F.; Calhorda, M. J. *Organometallics* **2005**, *24*, 1809−1812. (c) Jalon, F. A.; Lopez-Agenjo, A.; Manzano, B. R.; Moreno-Lara, M.; Rodriguez, A.; Sturm, T.; Weissensteiner, W. *J. Chem. Soc., Dalton Trans.* **1999**, *0*, 4031−4039.

(7) Jones, R. A.; Wilkinson, G.; Colquohoun, I. J.; McFarlane, W.; Galas, A. M. R.; Hursthouse, M. B. *J. Chem. Soc., Dalton Trans.* **1980**, 2480−2487.

(8) Lachaize, S.; Sabo-Etienne, S. *Eur. J. Inorg. Chem.* **2006**, 2115−2127.

(9) Alcaraz, G.; Sabo-Etienne, S. *Coord. Chem. Rev.* **2008**, *252*, 2395−2409.

(10) Ignatov, S. K.; Rees, N. H.; Tyrrell, B. R.; Dubberley, S. R.; Razuvaev, A. G.; Mountford, P.; Nikonov, G. I. *Chem.—Eur. J.* **2004**, *10*, 4991−4999.

(11) (a) Kubas, G. J. *Metal Dihydrogen and σ-Bond Complexes: Structure, Theory and Reactivity*; Kluwer Academic/Plenum Publishers: New York, 2001. (b) Besora, M.; Maseras, F.; Lledós, A.; Eisenstein, O. *Inorg. Chem.* **2002**, *41*, 7105−7112. (c) Kuramoto, Y.; Sawai, N.; Fujiwara, Y.; Sumimoto, M.; Nakao, Y.; Sato, H.; Sakaki, S. *Organometallics* **2005**, *24*, 3655−3663.

(12) (a) Schubert, U.; Ackermann, K.; Woerle, B. *J. Am. Chem. Soc.* **1982**, *104*, 7378−7380. (b) Tanaka, I.; Ohhara, T.; Niimura, N.; Ohashi, Y.; Jiang, Q.; Berry, D. H.; Bau, R. *J. Chem. Res., Synop.* **1999**, *14−15*, 180−192. (c) Bakhmutov, V. I.; Howard, J. A. K.; Keen, D. A.; Kuzmina, L. G.; Leech, M. A.; Nikonov, G. I.; Vorontsov, E. V.; Wilson, C. C. *Dalton* **2000**, *1631−1635*, 1153−1156. (d) Mork, B. V.; Tilley, T. D.; Schultz, A. J.; Cowan, J. A. *J. Am. Chem. Soc.* **2004**, *126*, 10428−10440. (e) McGrady, G. S.; Sirsch, P.; Chatterton, N. P.; Ostermann, A.; Gatti, C.; Altmannshofer, S.; Herz, V.; Eickerling, G.; Scherer, W. *Inorg. Chem.* **2009**, *48*, 1588−1598.

(13) (a) Hamilton, D. G.; Crabtree, R. H. *J. Am. Chem. Soc.* **1988**, *110*, 4126−4133. (b) Gründemann, S.; Limbach, H.-H.; Buntkowsky, G.; Sabo-Etienne, S.; Chaudret, B. *J. Phys. Chem. A* **1999**, *103*, 4752−4754.

(14) Balcells, D.; Clot, E.; Eisenstein, O. *Chem. Rev.* **2010**, *110*, 749−823.

(15) Panisch, R.; Bolte, M.; Müller, T. *J. Am. Chem. Soc.* **2006**, *128*, 9676−9682.

(16) Hoffmann, S. P.; Kato, T.; Tham, F. S.; Reed, C. A. *Chem. Commun.* **2006**, 767−769.

(17) Pertici, P.; Vitulli, G.; Paci, M.; Porri, L. *J. Chem. Soc., Dalton Trans.* **1980**, 1961−1964.

(18) Brookhart, M.; Grant, B.; Volpe, A. F. *Organometallics* **1992**, *11*, 3920−3922.

(19) (a) Becke, A. D. *J. Chem. Phys.* **1993**, *98*, 5648−5652. (b) Perdew, J. P.; Wang, Y. *Phys. Rev. B* **1992**, *45*, 13244−13249.

(20) Frisch, M. J.; Trucks, G. W.; Schlegel, H. B.; Scuseria, G. E.; Robb, M. A.; Cheeseman, J. R.; Montgomery, J. A., Jr.; Vreven, T.; Kudin, K. N.; Burant, J. C.; Millam, J. M.; Iyengar, S. S.; Tomasi, J.; Barone, V.; Mennucci, B.; Cossi, M.; Scalmani, G.; Rega, N.; Petersson, G. A.; Nakatsuji, H.; Hada, M.; Ehara, M.; Toyota, K.; Fukuda, R.; Hasegawa, J.; Ishida, M.; Nakajima, T.; Honda, Y.; Kitao, O.; Nakai, H.; Klene, M.; Li, X.; Knox, J. E.; Hratchian, H. P.; Cross, J. B.; Bakken, V.; Adamo, C.; Jaramillo, J.; Gomperts, R.; Stratmann, R. E.; Yazyev, O.; Austin, A. J.; Cammi, R.; Pomelli, C.; Ochterski, J. W.; Ayala, P. Y.; Morokuma, K.; Voth, G. A.; Salvador, P.; Dannenberg, J. J.; Zakrzewski, V. G.; Dapprich, S.; Daniels, A. D.; Strain, M. C.; Farkas, O.; Malick, D. K.; Rabuck, A. D.; Raghavachari, K.; Foresman, J. B.; Ortiz, J. V.; Cui, Q.; Baboul, A. G.; Clifford, S.; Cioslowski, J.; Stefanov, B. B.; Liu, G.; Liashenko, A.; Piskorz, P.; Komaromi, I.; Martin, R. L.; Fox, D. J.; Keith, T.; Al-Laham, M. A.; Peng, C. Y.; Nanayakkara, A.; Challacombe, M.; Gill, P. M. W.; Johnson, B.; Chen, W.; Wong, M. W.; Gonzalez, C.; Pople, J. A. In *Gaussian 03*; Gaussian, Inc.: Wallingford, CT, 2004.

(21) (a) Andrae, D.; Häussermann, U.; Dolg, M.; Stoll, H.; Preuss, H. *Theor. Chim. Acta* **1990**, *77*, 123−141. (b) Bergner, A.; Dolg, M.; Küchle, W.; Stoll, H.; ; Preuss, , H. *Mol. Phys.* **1993**, *80*, 1431−1441.

(22) (a) Ehlers, A. W.; Böhme, M.; Dapprich, S.; Gobbi, A.; Höllwarth, A.; Jonas, V.; Köhler, K. F.; Stegmann, R.; Veldkamp, A.; Frenking, G. *Chem. Phys. Lett.* **1993**, *208*, 111−114. (b) Höllwarth, A.; Böhme, M.; Dapprich, S.; Ehlers, A. W.; Gobbi, A.; Jonas, V.; Köhler, K. F.; Stegmann, R.; Veldkamp, A.; Frenking, G. *Chem. Phys. Lett.* **1993**, *208*, 237−240.

(23) Hariharan, P. C.; Pople, J. A. *Theor. Chim. Acta* **1973**, *28*, 213−222.

(24) Archer, J. M.; Lehmann, M. S. *J. Appl. Crystallogr.* **1986**, *19*, 456−458.

(25) Buffet, J. C.; Clergeau, J. F.; Cooper, R. G.; Darpentigny, J.; De Laulany, A.; Fermon, C.; Fetal, S.; Fraga, F.; Guerard, B.; Kampmann, R.; Kastenmueller, A.; McIntyre, G. J.; Manzin, G.; Meilleur, F.; Millier, F.; Rhodes, N.; Rosta, L.; Schooneveld, E.; Smith, G. C.; Takahashi, H.; Van Esch, P.; Van Vuure, T. L.; Zeitelhack, K. *Nuclear Instrum. Methods Phys. Res., Sect. A* **2005**, *554*, 392−405.